Journal of Oceanography, Vol. 65, pp. 689 to 701, 2009

Seasonal and Interannual Variability of Oceanic Carbon Cycling in the Western and Central Tropical–Subtropical Pacific: A Physical-Biogeochemical Modeling Study

Masahiko Fujii[1,2]*, Fei Chai[3], Lei Shi[3], Hisayuki Y. Inoue[1] and Masao Ishii[4]

[1]*Graduate School of Environmental Science, Hokkaido University, Sapporo, Hokkaido 060-0810, Japan*
[2]*Sustainability Governance Project, Center for Sustainability Science, Hokkaido University, Sapporo, Hokkaido 060-0809, Japan*
[3]*School of Marine Sciences, 5706 Aubert Hall, University of Maine, Orono, ME 04469-5706, U.S.A.*
[4]*Meteorological Research Institute, Nagamine, Tsukuba, Ibaraki 305-0052, Japan*

(Received 4 October 2008; in revised form 7 July 2009; accepted 20 July 2009)

The oceanic carbon cycle in the tropical–subtropical Pacific is strongly affected by various physical processes with different temporal and spatial scales, yet the mechanisms that regulate air–sea CO_2 flux are not fully understood due to the paucity of both measurement and modeling. Using a 3-D physical-biogeochemical model, we simulate the partial pressure of CO_2 in surface water (pCO_{2sea}) and air–sea CO_2 flux in the tropical and subtropical regions from 1990 to 2004. The model reproduces well the observed spatial differences in physical and biogeochemical processes, such as: (1) relatively higher sea surface temperature (SST), and lower dissolved inorganic carbon (DIC) and pCO_{2sea} in the western than in the central tropical–subtropical Pacific, and (2) predominantly seasonal and interannual variations in the subtropical and tropical Pacific, respectively. Our model results suggest a non-negligible contribution of the wind variability to that of the air–sea CO_2 flux in the central tropical Pacific, but the modeled contribution of 7% is much less than that from a previous modeling study (30%; McKinley *et al.*, 2004). While DIC increases in the entire region, SST increases in the subtropical and western tropical Pacific but decreases in the central tropical Pacific from 1990 to 2004. As a result, the interannual pCO_{2sea} variability is different in different regions. The pCO_{2sea} temporal variation is found to be primarily controlled by SST and DIC, although the role of salinity and total alkalinity, both of which also control pCO_{2sea}, need to be elucidated by long-term observations and eddy-permitting models for better estimation of the interannual variability of air–sea CO_2 flux.

Keywords:
· Carbon cycling,
· physical-biogeochemical model,
· tropical–subtropical Pacific.

1. Introduction

The tropical Pacific is the largest natural ocean CO_2 source to the atmosphere (e.g. Tans *et al.*, 1990; Takahashi *et al.*, 1997, 1999; Feely *et al.*, 2004). The biogeochemistry in the tropical Pacific is primarily controlled by the mean circulation whereby upwelling brings cold, nutrient- and carbon-rich subsurface water to the surface (e.g. Toggweiler and Carson, 1995; Feely *et al.*, 2006). As a result, sea-to-air CO_2 efflux is strengthened or weakened by the degree of upwelling on various time scales, such as El Niño Southern Oscillation (ENSO), Pacific Decadal Oscillation (PDO), tropical instability waves, Kelvin waves and global warming (e.g. Barber *et al.*, 1996; Foley *et al.*, 1996; Dunne *et al.*, 1999). The tropical Pacific is a major source of CO_2 to the atmosphere (0.8–1.0 PgC yr^{-1}) during non-El Niño periods but near neutral (0.2–0.4 PgC yr^{-1}) during strong El Niño periods (e.g. Feely *et al.*, 1995, 1997, 1999; Ishii *et al.*, 2004).

The tropical Pacific can be divided into two distinct provinces: the Western Pacific Warm Pool (WPWP) which is usually characterized by high sea surface temperature (SST > 28.5°C), low sea surface salinity (SSS < 34.5 psu), low surface nutrients and dissolved inorganic carbon (DIC) (e.g. Takahashi *et al.*, 2003; Ishii *et al.*, 2009), and

* Corresponding author. E-mail: mfujii@ees.hokudai.ac.jp

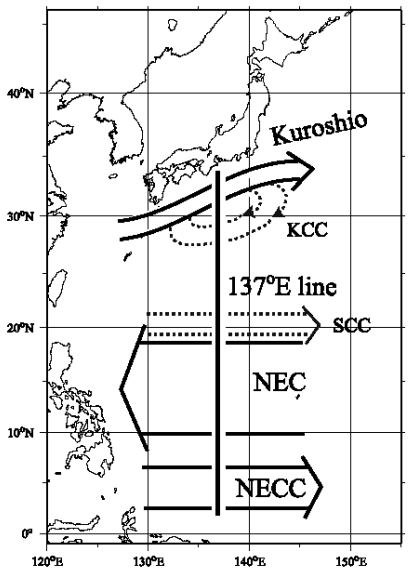

Fig. 1. Locations of the observation line and major currents along 137°E in the western North Pacific. Abbreviations: KCC, Kuroshio Counter-Current; SCC, Subtropical Counter-Current; NEC, North Equatorial Current; NECC, North Equatorial Counter-Current (figure from Midorikawa *et al.*, 2005).

the central tropical Pacific or the Pacific Equatorial Divergence (PED) marked as lower SST, higher SSS, higher surface nutrients and DIC, higher primary production, and higher pCO_{2sea}. The partial pressure of CO_2 in the surface water (pCO_{2sea}) in the WPWP is similar to or slightly higher than that in the atmosphere (pCO_{2air}). The higher surface nutrients and DIC in the PED are caused by upwelling of subsurface water, and also due to lack of iron (Barber, 1992). pCO_{2sea} in the PED is reduced by the effect of lower SST but is high because of high DIC, and as a result, the PED is usually characterized by a strong source of CO_2 to the atmosphere (Feely *et al.*, 2006). There are significant horizontal differences in the oceanic carbon cycling and biogeochemical responses to ENSO that are associated with the change in the expanse of WPWP and PED (Inoue *et al.*, 1996; Le Borgne *et al.*, 2002).

The subtropical Pacific is known to undergo significant changes on seasonal, interannual (ENSO), and decadal (PDO) time scales. The western subtropical Pacific, in particular, has complex current structures: westward North Equatorial Current, eastward Subtropical Counter-Current, Kuroshio Counter-Current, and eastward Kuroshio Current, from south to north (e.g. Fig. 1; Midorikawa *et al.*, 2005). The biogeochemical processes are affected by the strength of these currents with various time scales. Along with the hydrographic properties, the DIC and pCO_{2sea} in the surface waters of the western North Pacific subtropical gyre between the tropical region and the Kuroshio Current (3–34°N) have been measured for decades (e.g. Inoue *et al.*, 1987, 1995; Ishii *et al.*, 2001, 2009; Midorikawa *et al.*, 2005). A long-term increase in pCO_{2sea} along 137°E has been observed in winter. The growth rate since 1984 between 15°N and 30°N is estimated to be 1.7 ± 0.2 (μatm yr^{-1}), which is similar to the growth rate of pCO_{2air}.

While the factors that regulate air–sea CO_2 flux have been regularly explored by previous observers, the temporal and spatial variability of the carbon cycle in the tropical–subtropical Pacific has not yet been elucidated in a comprehensive fashion, and the processes controlling pCO_{2sea} variation are not fully understood (Ishii *et al.*, 2001). Especially across most of the Pacific, data for quantification of interannual variability and long-term trends are relatively sparse (McKinley *et al.*, 2006).

Modeling can help us to fill the gaps in observations and interpret observed results. A number of diagnostic and 3-D ocean modeling studies examined the air–sea exchange of CO_2 in the tropical Pacific (e.g. Winguth *et al.*, 1994; Le Quéré *et al.*, 2000; Obata and Kitamura, 2003; McKinley *et al.*, 2004, 2006; Park *et al.*, 2006). Several modeling studies suggest that the global air–sea CO_2 flux interannual variability is largely (nearly 70%) driven by the tropical Pacific (e.g. Winguth *et al.*, 1994; Le Quéré *et al.*, 2000; Obata and Kitamura, 2003; Park *et al.*, 2006).

Although several pioneering modeling studies have begun to treat the oceanic carbon cycling and the marine ecosystem dynamics simultaneously in their models (e.g. Jiang and Chai, 2006; McKinley *et al.*, 2006; Wang *et al.*, 2006; Fujii and Chai, 2007; Fujii and Yamanaka, 2008), very few previous modeling studies have applied their marine ecosystem models to, or have compared model results with, observations in the northwestern part of the tropical–subtropical Pacific. In this study, we use a physical-biogeochemical model, incorporating the oceanic carbon cycling and air–sea CO_2 exchange, to examine temporal variations in each basin, especially focusing on the seasonal and interannual variations and east–west comparison in the tropical and subtropical Pacific. The model framework and experimental design are explained in the next section. The modeled seasonal and interannual variations of SST, SSS, DIC, total alkalinity (TA), pCO_{2sea} and air–sea CO_2 flux are described in Section 3. Section 4 focuses on discussing the question which are the predominant factors controlling the pCO_{2sea} and air–sea CO_2 flux in each region of the tropical–subtropical Pacific, especially stressing the significant effects of the SST and DIC on the spatiotemporal variations of the pCO_{2sea} and air–sea CO_2 flux. Section 5 summarizes the results obtained in this study.

2. Model Description and Experimental Design

We use a biogeochemical model (Carbon, Silicate, Nitrogen Ecosystem (CoSINE) Model; Chai *et al*., 2002; Dugdale *et al*., 2002) to examine spatial and temporal variations of pCO_{2sea} and air–sea CO_2 flux and their causes for each basin. The model consists of two phytoplankton functional groups (picoplankton and diatoms), three zooplankton (microzooplankton, mesozooplankton and predatory zooplankton), three nutrients (nitrate, ammonium and silicic acid), detritus (particulate organic nitrogen and carbon, and biogenic silica), and DIC.

The linkage of the carbon cycle to the ecosystem components is through the consumption and remineralization of assimilated nutrients based upon the nitrogen changes in the water column by using Redfield stoichiometric ratios (Chai *et al*., 2002). The C/N ratio of 117/16 (=7.3) of Anderson and Sarmiento (1994) is used. Instead of modeling the distribution of alkalinity in the water column, surface TA is determined only by a statistical regional representation of salinity normalized alkalinity (Millero *et al*., 1998). The representation of SST, SSS, DIC and TA in the model allows us to calculate pCO_{2sea} and air–sea CO_2 flux.

The biogeochemical model is coupled with the Regional Ocean Modeling System (ROMS) (e.g. Chai *et al*., 2003, 2009; Wang and Chao, 2004; Liu and Chai, 2009). The model is focused on the Pacific Ocean and its domain is 45°S to 65°N, 99°E to 70°W. The spatial resolution is 0.5° × 0.5°. See Liu and Chai (2009) and Chai *et al*. (2009) for details.

The coupled physical-biogeochemical model is forced by the wind obtained from the National Centers for Environmental Prediction (NCEP) reanalysis data (Kalnay *et al*., 1996). The Ocean Carbon-Cycle Model Intercomparison (OCMIP)'s CO_2 system (Orr, 1996), the monthly *in situ* observational data of the partial pressure of CO_2 in the atmosphere (pCO_{2air}) at Mauna Loa (Keeling *et al*., 1982; Conway *et al*., 1994), and Wanninkhof's (1992) gas exchange parameterization are used to calculate the air–sea CO_2 flux. Model results for 1990 to 2004 are discussed in this study.

The model performance is validated by comparing its results to observational data from the following: the Japan Meteorological Agency (JMA)/Meteorological Research Institute (MRI) for the western tropical and subtropical Pacific (Fig. 1; Inoue *et al*., 1995, 2001; Ishii *et al*., 2004; Midorikawa *et al*., 2005); the National Oceanic and Atmospheric Administration (NOAA)/Pacific Marine Environmental Laboratory (PMEL) cruises that service the Tropical Ocean-Global Atmosphere (TOGA)-Tropical Atmosphere Ocean (TAO) Array (Feely *et al*., 2002, 2006; Cosca *et al*., 2003) for the central tropical Pacific; the observations at Station ALOHA (22.75°N, 158.00°W), the location of the U.S. JGOFS Hawaii Ocean Time-series (HOT) program (Karl and Lukas, 1996; Dore *et al*., 2003; Brix *et al*., 2004; Keeling *et al*., 2004) for the central subtropical Pacific. The data at the Carbon Dioxide Information and Analysis Center (CDIAC) at the Oak Ridge National Laboratory, Oak Ridge, TN (LDEO database NDP-088; Takahashi *et al*., 2002, 2008, 2009) are also used to verify the model results in the entire oceanic region.

The pCO_{2sea} is dependent upon the surface temperature, salinity, DIC and TA. To diagnose the factors driving the variability in modeled pCO_{2sea}, the effects on pCO_{2sea} of SST, SSS, DIC and TA may be written in linearized form (Takahashi *et al*., 1993; Le Quéré *et al*., 2000; McKinley *et al*., 2004, 2006):

$$\frac{d\mathrm{pCO_{2sea}}}{dt} = \frac{\partial \mathrm{pCO_{2sea}}}{\partial \mathrm{SST}} \frac{d\mathrm{SST}}{dt} + \frac{\partial \mathrm{pCO_{2sea}}}{\partial \mathrm{SSS}} \frac{d\mathrm{SSS}}{dt} + \frac{\partial \mathrm{pCO_{2sea}}}{\partial \mathrm{DIC}} \frac{d\mathrm{DIC}}{dt} + \frac{\partial \mathrm{pCO_{2sea}}}{\partial \mathrm{TA}} \frac{d\mathrm{TA}}{dt}. \quad (1)$$

Separation of these multiple influences allows a more detailed understanding of the surface ocean carbon cycle and of the model's representation of these processes (McKinley *et al*., 2006). The four partial differential terms in the waters have been determined experimentally or computed using thermodynamic relationships (Takahashi *et al*., 1993).

3. Results

3.1 Seasonal variability

The observations indicate that there is a strong contrast between the western and central Pacific (e.g. Inoue *et al*., 2001). The annual-mean model results averaged over 1990–2004 show relatively higher SST, lower SSS, lower DIC, and generally lower pCO_{2sea} and lower wind speed in the western Pacific than in the central Pacific (Fig. 2). SST and pCO_{2sea} decrease and DIC increases monotonically with latitude toward the north along 137°E, as has been observed by Midorikawa *et al*. (2005), while along 155°W the SST has a minimum, and DIC and pCO_{2sea} have maxima, at the equator. The modeled annual sea-to-air CO_2 flux shows that the subtropical region north of 25°N along 137°E functions as a large sink for atmospheric CO_2 (Fig. 2), as was observed by Midorikawa *et al*. (2005). The tropical region south of 9°N along 137°E functions as a weak source (0.49 mmolC $m^{-2}yr^{-1}$ on average). The model overestimates observationally based estimates of 0.06–0.28 mmolC $m^{-2}yr^{-1}$ (Ishii and Inoue, 1995; Takahashi *et al*., 2002, 2008, 2009). Along 155°W, the ocean functions as a strong source of atmospheric CO_2 around the equator, and a sink between 8°N and 31°N.

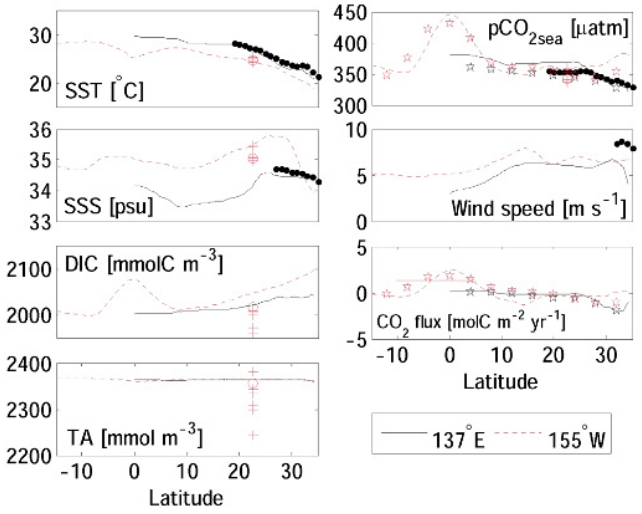

Fig. 2. Modeled latitudinal profiles of annual-mean SST, SSS, surface DIC and TA, pCO_{2sea}, wind speed and sea-to-air CO_2 flux, along 137°E (in solid black lines) and 155°W (in dotted red lines). A red solid line for CO_2 flux and red open circles denote observational results in the tropical central Pacific (Cosca *et al.*, 2003) and at Station ALOHA (Keeling *et al.*, 2004), respectively. Stars denote data from Takahashi *et al.* (2002, 2008, 2009). Red crosses denote seven model results shown in McKinley *et al.* (2006): ROMS-Maine (Chai *et al.*, 2002, 2003), MIT (McKinley *et al.*, 2004), UMD (Christian *et al.*, 2002), NCOM-Maine (Jiang and Chai, 2005), BEC-CCCSM (Moore *et al.*, 2004), MPI-Met (Wetzel *et al.*, 2005) and PISCES-T (Buitenhuis *et al.*, 2006).

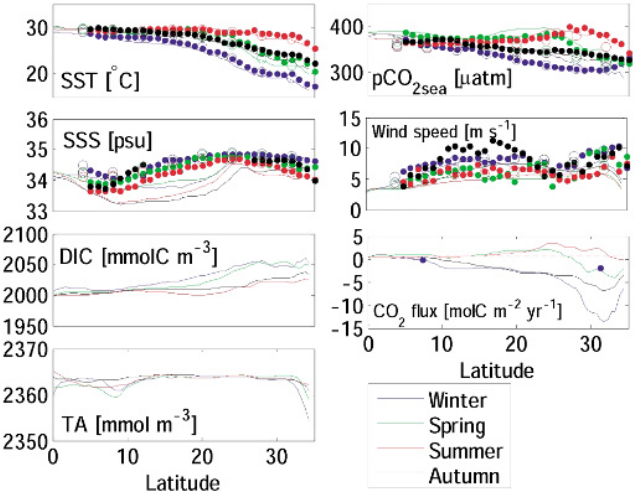

Fig. 3-1. Latitudinal profiles of seasonal-mean SST, SSS, surface DIC and TA, pCO_{2sea}, wind speed and sea-to-air CO_2 flux in winter (in blue), spring (in green), summer (in red) and autumn (black), along 137°E. Solid lines denote model results. Other lines or symbols show observational data: open circles from Takahashi *et al.* (2002, 2008, 2009), solid dots from Midorikawa *et al.* (2005). Dashed line is sea-to-air CO_2 flux from Ishii *et al.* (2001).

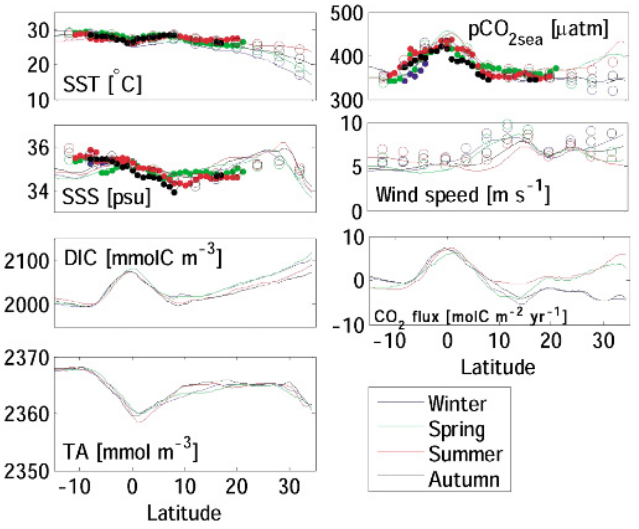

Fig. 3-2. Same as in 3-1 but for along 155°W. Dots show observational data: open dots from Takahashi *et al.* (2002, 2008, 2009) and solid dots from Feely *et al.* (2002).

The seasonal (three month) mean model results averaged over 1990–2004 also reproduce well the observed seasonal patterns of SST, SSS, DIC, pCO_{2sea}, wind speed and sea-to-air CO_2 flux along 137°E and 155°W (Figs. 3-1 and 3-2). The seasonal amplitude, which is defined as the difference between the climatological annual maximum and minimum, generally increases with latitude both along 137°E and 155°W for all model fields (Fig. 4).

Along 137°E, SST decreases monotonically with latitude all year round (Fig. 3-1), which is similar to the observed trends (see Midorikawa *et al.*, 2005). The seasonal amplitude of SST is 3.4°C at 15°N and 8.7°C at 25°N (Fig. 4). This is consistent with observations (3.5 ± 1.5°C between 7–20°N and 8.5 ± 3.5°C between 20–30°N; Ishii *et al.*, 2001). DIC increases monotonically with latitude, and the latitudinal gradient is greater in winter and spring than in the other two seasons (Fig. 3-1). The seasonal amplitude of DIC is 19.1 mmolC m^{-3} at 15°N and 52.3 mmolC m^{-3} at 25°N (Fig. 4), consistent or slightly higher compared to observations (13 ± 6 mmolC m^{-3} between 7–20°N, and 26 ± 13 mmolC m^{-3} between 20–30°N; Ishii *et al.*, 2001). pCO_{2sea} decreases monotonically with latitude in winter and autumn (Fig. 3-1), as observed by Midorikawa *et al.* (2005). The maximum pCO_{2sea} occurs at around 25°N in spring and summer, resulting from both high SST and DIC in this oceanic region in spring and summer. In the tropical region south of 6°N, slightly posi-

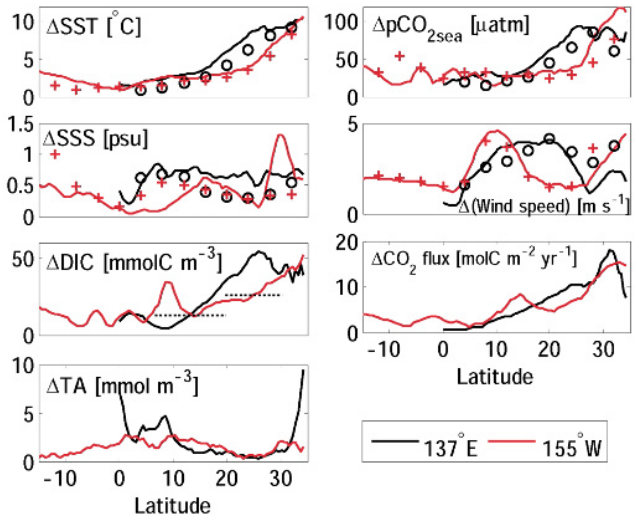

Fig. 4. Modeled latitudinal profiles of seasonal amplitudes of SST, SSS, surface DIC and TA, pCO_{2sea}, wind speed and sea-to-air CO_2 flux, along 137°E (black) and 155°W (red). Black open circles and red crosses show observational data along 137°E and 155°W, respectively, from Takahashi *et al*. (2002, 2008, 2009). Dotted black lines denote observational results along 137°E from Ishii *et al*. (2001).

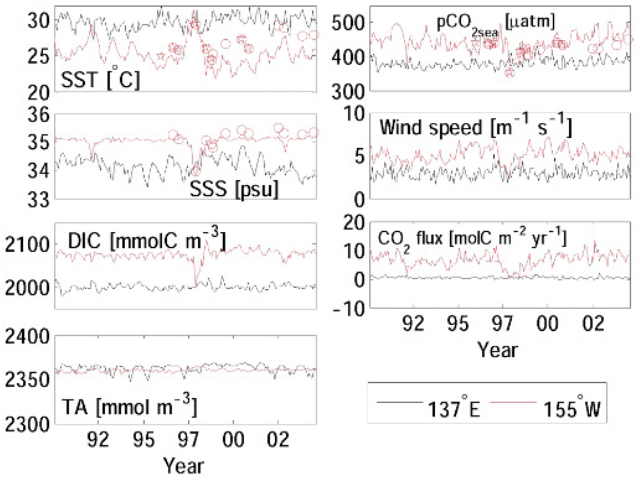

Fig. 5-1. Interannual variations of SST, SSS, surface DIC and TA, pCO_{2sea}, wind speed and sea-to-air CO_2 flux from 1990 to 2004 at 0°N, along 137°E (in black) and 155°W (in red). Symbols and lines denote observational data (red open circles from Feely *et al*., 2002, and red stars from Cosca *et al*., 2003) and model results, respectively.

tive ΔpCO_2 (pCO_{2sea} minus pCO_{2air}) is maintained throughout the year, consistent with the observations (by 0–10 μatm between 3°N and 6°N; Midorikawa *et al*., 2005). In the subtropical region, on the other hand, the pCO_{2sea} is much lower than pCO_{2air} in winter and autumn,

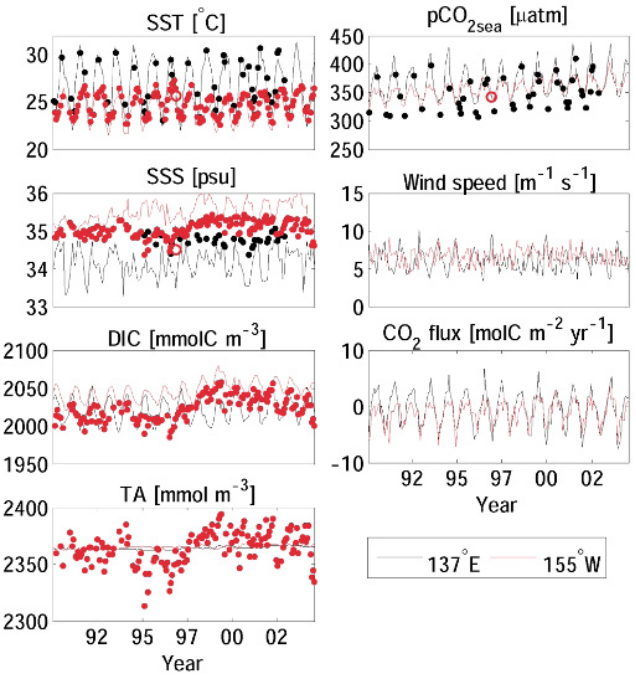

Fig. 5-2. Same as in 5-1 but for 22.5°N. Black and red solid dots denote observational data from Inoue *et al*. (2001) and from Brix *et al*. (2004), respectively.

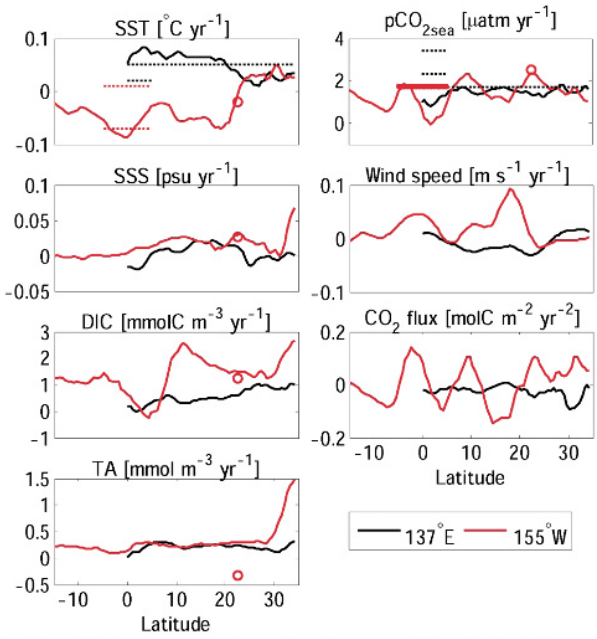

Fig. 6. Modeled latitudinal profiles of interannual change rates from 1990 to 2004 for SST, SSS, surface DIC and TA, pCO_{2sea}, wind speed and sea-to-air CO_2 flux, along 137°E (black solid lines) and 155°W (red solid lines). Red open dots denote observational results at Station ALOHA (Keeling *et al*., 2004). Dotted lines show observational results along 137°E (in black; from Takahashi *et al*., 2003; Midorikawa *et al*., 2005) and 155°W (in red; from Feely *et al*., 2006).

especially immediately south of the Kuroshio (>30°N), which is consistent with previous observation-based reports (60 μatm difference north of 25°N in winter; e.g. Inoue *et al*., 1987, 1995; Murata and Fushimi, 1996; Ishii *et al*., 2001; Midorikawa *et al*., 2005).

The modeled latitudinal profiles of SST and DIC in the subtropical region north of 10°N are similar between 137°E and 155°W (Figs. 3-1 and 3-2), although the seasonal amplitudes are larger along 137°E (Fig. 4). pCO_{2sea} in the subtropical region along 155°W increases with latitude (Fig. 2), especially in spring and summer (Fig. 3-2). The latitudinal profile of pCO_{2sea} in the subtropical region is very different between 137°E and 155°W (Figs. 2, 3-1 and 3-2). This mainly results from differences in the contribution of SST and DIC to pCO_{2sea} between 137°E and 155°W, as explained in Subsection 4.1. Along 155°W, a minimum of SST, and maxima of DIC and pCO_{2sea}, always appear near the equator, which are not present along 137°E (Figs. 2, 3-1 and 3-2). ΔpCO_2 is as high as 90 μatm near the equator along 155°W.

Along 137°E, the net sea-to-air CO_2 flux in the tropical regions south of 9°N is slightly positive during all four seasons (Fig. 3-1). Modeled sea-to-air CO_2 flux in the subtropical regions north of 9°N is slightly positive, 1.4 molC $m^{-2}yr^{-1}$, in the summer, which is close to an observation-based estimate of about 1.5 molC $m^{-2}yr^{-1}$ (Ishii *et al*., 2001). The flux is strongly negative in autumn and winter, becoming more negative toward the north, 0.4 molC $m^{-2}yr^{-1}$ at 5°N, –0.1 molC $m^{-2}yr^{-1}$ at 7°N and –13.1 molC $m^{-2}yr^{-1}$ at 31°N in winter, which are close to the observations (no more than 0.2 ± 0.2 molC $m^{-2}yr^{-1}$ at 3–6°N, –0.1 ± 0.2 molC $m^{-2}yr^{-1}$ at 7°N and –5.1 ± 0.7 molC $m^{-2}yr^{-1}$ at 31°N; Midorikawa *et al*., 2005). The net air-to-sea CO_2 flux in the subtropical regions (7–34°N) in winter accounts for 39% of the annual influx, close to an observation-based estimate of 40–60% (Midorikawa *et al*., 2005). Along 155°W, by contrast, a strong sea-to-air CO_2 flux is seen in the tropical region all year round (Fig. 3-2). The role of the subtropical ocean north of 10°N in the air–sea CO_2 exchange differs with the season: it functions as a source of atmospheric CO_2 in the summer, becoming more so with increasing latitude, and as a sink in the autumn and winter.

3.2 Interannual variability

Previous observational and modeling studies have elucidated that there is substantial interannual variability both in physical and biogeochemical processes in the tropical and subtropical Pacific (e.g. Inoue *et al*., 2001; Feely *et al*., 2002; Takahashi *et al*., 2002; Cosca *et al*., 2003; Brix *et al*., 2004; McKinley *et al*., 2006). The model results reproduce the observed interannual variability from 1990 through 2004, very well for the SST along both 137°E and 155°W and the SSS and pCO_{2sea} along 155°W, and reasonably well for the DIC along 155°W (at Station ALOHA) and the pCO_{2sea} along 137°E (Figs. 5-1 and 5-2), although further model-data comparison is required for more detailed evaluation. Interannual variability is more significant in the tropics than in the subtropics, and more pronounced in the central equatorial Pacific (along 155°W) than along 137°E, primarily induced by the ENSO events, which is consistent with the observational results (e.g. Inoue *et al*., 2001; Feely *et al*., 2002).

While the model captures the observed sudden El Niño-induced decrease in SSS at the equator at the end of 1997, it fails to reproduce the substantial freshening that occurred around Station ALOHA from approximately 1995–1997 that Brix *et al*. (2004) suggest is due to water mass changes. None of the previous models succeed in reproducing the decrease in SSS at ALOHA. Damped salinity variability and limited physical variability due to the lack of explicit mesoscale eddies and model boundary conditions provide some explanation for the model's failure with respect to the observed variations (McKinley *et al*., 2006).

The rate of increase of each component averaged at each 1° in latitude along 137°E and 155°W is calculated using linear least squares for the simulation period from 1990 to 2004 (Fig. 6). Modeled SST along 137°E increases by 0.05 ± 0.02°C yr^{-1} on average north of the equator, and by 0.07 ± 0.01 and 0.04 ± 0.02°C yr^{-1} in the tropical and subtropical regions, respectively (Fig. 6). This estimate is slightly higher than observation-based estimates of 0.02 ± 0.02°C yr^{-1} along 137°E (Midorikawa *et al*., 2005) and in the western tropical Pacific (Takahashi *et al*., 2003). The decrease in modeled SST along 155°W is 0.02 ± 0.04°C yr^{-1} on average north of the equator, or 0.04 ± 0.02 and 0.01 ± 0.04°C yr^{-1} in the tropical and subtropical regions, respectively. This is roughly consistent with observations in the central tropical Pacific in which the decrease was estimated to be by 0.07 ± 0.04°C yr^{-1} (Takahashi *et al*., 2003). Modeled DIC increases in the entire region, both along 137°E and 155°W (Fig. 6), consistent with observations (e.g. 1.22 ± 0.14 mmolC $m^{-3}yr^{-1}$; Dore *et al*., 2003). The modeled rate of increase north of the equator is greater along 155°W than along 137°E, at 1.45 ± 0.77 and 0.58 ± 0.29 mmolC $m^{-3}yr^{-1}$, respectively.

The modeled rate of increase of pCO_{2sea} north of the equator along 137°E ranges from 0.8 to 1.8 μatm yr^{-1} (Fig. 6). The mean increase rate is 1.3 ± 0.3 μatm yr^{-1} in the tropical region, 1.5 ± 0.1 μatm yr^{-1} in the subtropical region and 1.5 ± 0.2 μatm yr^{-1} on average in the entire region. The rate is close to an observation-based result of 1.7 ± 0.2 μatm yr^{-1} (Midorikawa *et al*., 2005), although observed rates of increase that exceeded 2.0 μatm yr^{-1} in the tropical region (3°N to 6°N) and at the northernmost latitude of 34°N (Midorikawa *et al*., 2005) are not seen

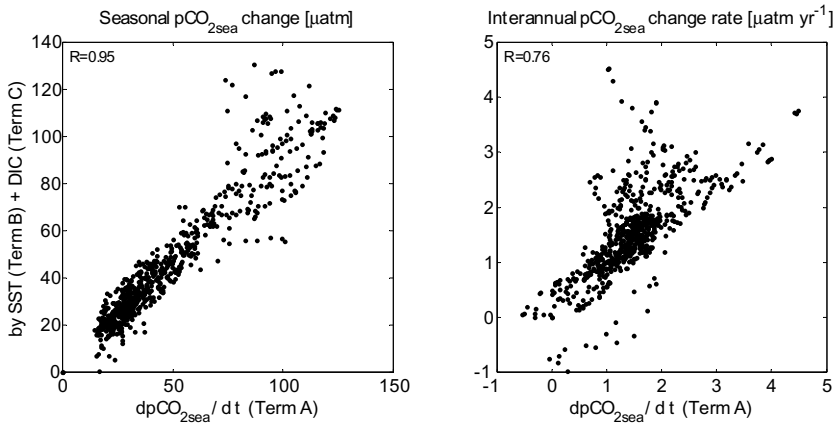

Fig. 7. Modeled seasonal and interannual pCO_{2sea} change rates, by SST (Term B) and surface DIC (Term C) vs. by SST, SSS, surface DIC and TA (Term A), respectively, as shown in Eq. (2). See text for exact definition of Terms A–C.

in the model. The modeled rate of increase of pCO_{2sea} north of the equator along 155°W ranges from 0.0 to 2.4 μatm yr^{-1}. The increase rate is 0.9 ± 0.8 μatm yr^{-1} in the tropical region, 1.6 ± 0.4 μatm yr^{-1} in the subtropical region and 1.4 ± 0.6 μatm yr^{-1} on average in the entire region, close to an observation-based estimate of 1.8 ± 0.7 μatm yr^{-1} in the tropical region from 5°S to 5°N (Takahashi *et al*., 2003).

While the modeled pCO_{2sea} increases in the entire region from 1990 to 2004, the modeled sea-to-air CO_2 flux is unchanged or even decreased in the subtropical regions, by –0.07 ± 0.07 mmolC m^{-2}yr^{-2} along 137°E and by 0.03 ± 0.22 mmolC m^{-2}yr^{-2} along 155°W (Fig. 6). This is consistent with observational results along 137°E (Midorikawa *et al*., 2005) which showed that the net air-to-sea CO_2 flux in winter remained at a similar level in the subtropical regions from 7–34°N. Midorikawa *et al*. (2005) argue that the flux has remained at fairly similar levels for the past two decades over the zones north of 7°N along 137°E because of the insignificant long-term changes in both ΔpCO_2 (pCO_{2sea} minus pCO_{2air}; –0.3 ± 0.3 to 0.3 ± 0.3 μatm yr^{-1}) and wind speed. The model results in the subtropical region show insignificant long-term changes in ΔpCO_2 (–0.16 ± 0.13 and –0.06 ± 0.40 μatm yr^{-1} along 137°E and 155°W, respectively) and in wind speed (–0.01 ± 0.02 and 0.02 ± 0.03 m s^{-1}yr^{-1} along 137°E and 155°W, respectively), supporting their conclusion. The model results in the tropical regions along 137°E show a slight decrease in ΔpCO_2 (–0.40 ± 0.30 μatm yr^{-1}), inconsistent with the wintertime observation (Midorikawa *et al*., 2005) which reported an increase in ΔpCO_2 of around 0.5 μatm yr^{-1}. This discrepancy leads to different results in the long-term change in sea-to-air CO_2 flux in the tropical region along 137°E, i.e., a slight increase by the observation (Midorikawa *et al*., 2005) and a slight decrease of 0.05 ± 0.02 mmolC m^{-2}yr^{-2} in the model. The observation along 137°E has been previously carried out only in winter and has not covered all the seasons. Whether the model-data misfits in the sea-to-air CO_2 flux in the tropical region along 137°E are alleviated by using more realistic physical-biogeochemical models or by applying seasonally-covered data for comparison will be clarified in future work.

The modeled sea-to-air CO_2 flux variation from 1990 to 2004 in the tropical region along 155°W is estimated to be –0.03 ± 0.15 mmolC m^{-2}yr^{-2} and does not show a strong trend. The interannual variations in the central tropical Pacific are caused predominantly by the ENSO, and will be discussed in detail in Subsection 4.2.

4. Discussion

4.1 Factors driving seasonal and interannual variability of pCO_{2sea}

As shown in the previous section, pCO_{2sea} varies in concert with spatiotemporal variations of SST, SSS, DIC and TA, especially with SST and DIC. The separation of multiple influences that affect pCO_{2sea} variation allows a more detailed understanding of the surface ocean carbon cycle and of the model's representation of these processes (McKinley *et al*., 2006). The contribution of each factor to the pCO_{2sea} variation is calculated as described in Eq. (1). We found that the effects of SSS and TA on the pCO_{2sea} change are relatively small in this study, so Eq. (1) can be rewritten approximately as

$$\underbrace{\frac{d\mathrm{pCO_{2sea}}}{dt}}_{\text{Term A}} \approx \underbrace{\frac{\partial \mathrm{pCO_{2sea}}}{\partial \mathrm{SST}}\frac{d\mathrm{SST}}{dt}}_{\text{Term B}} + \underbrace{\frac{\partial \mathrm{pCO_{2sea}}}{\partial \mathrm{DIC}}\frac{d\mathrm{DIC}}{dt}}_{\text{Term C}}. \quad (2)$$

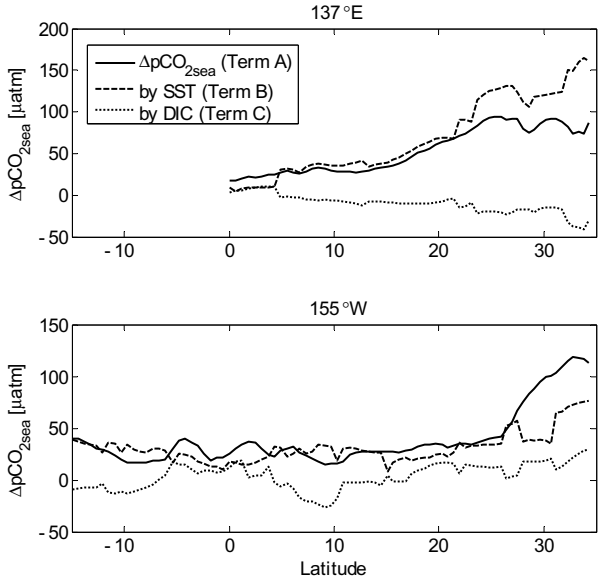

Fig. 8. Modeled latitudinal profiles of seasonal amplitude of ΔpCO_{2sea} (solid lines), and the effects of SST (dashed lines) and surface DIC (dotted lines) on its seasonal amplitude, along 137°E and 155°W.

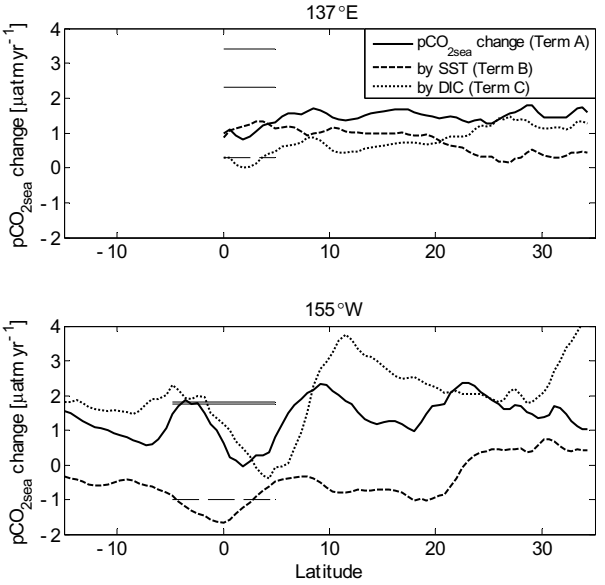

Fig. 9. Modeled latitudinal profiles of interannual change rate of pCO_{2sea} (in bold solid lines), and the effect of SST (in bold dashed lines) and surface DIC (in bold dotted lines) on its interannual change rate, along 137°E and 155°W. Light solid and dashed lines show observed interannual change rate of pCO_{2sea} and the effect of SST, respectively (Takahashi *et al*., 2003; Feely *et al*., 2006).

The term on the left hand side, and the first and second terms on the right hand side, are called Terms A, B, and C respectively, hereafter and in Fig. 7. Figure 7 shows that the right hand side of Eq. (2) can account for 95% and 76% of the seasonal and interannual pCO_{2sea} change, respectively. The relatively weak correlation between the left and right hand sides of Eq. (2) in the interannual pCO_{2sea} change implies that SSS and/or TA play an additional role in determining the interannual pCO_{2sea} variability.

The model results show that the seasonal change in pCO_{2sea} is mainly determined by the seasonal change in SST and DIC at each latitude and longitude (Figs. 7 and 8). Along 137°E (Fig. 8), the effect of seasonal SST variability is partially cancelled out by that of seasonal DIC variability, by 21% and 15% at 15°N and 25°N, respectively. The offset is smaller in the model than in an observation-based deduction that the effect of seasonal DIC variability cancelled out that of seasonal SST variability by 50% (between 7–20°N) and 30% (between 20–30°N) (Ishii *et al*., 2001). Along 155°W (Fig. 8), the effect of seasonal DIC variability cancels out that of seasonal SST variability by 30% south of 6°S and between 4°N and 14°N. At other latitudes, the seasonal changes in SST and DIC contribute in the same direction to the seasonal variation in pCO_{2sea}. In particular, pCO_{2sea} variation in the subtropical region north of 14°N is highlighted by the lowest DIC and pCO_{2sea} in the autumn (Fig. 3-2). The pCO_{2sea} variation near Station ALOHA is primarily temperature-controlled, which agrees with observational results (Keeling *et al*., 2004; McKinley *et al*., 2006).

The interannual pCO_{2sea} variation is also strongly controlled by the SST and DIC variations, although neglect of the other controlling factors of SSS and TA is considered to be less appropriate than in the case of the seasonal variation (Fig. 7), as mentioned above. The model results show that the increase of pCO_{2sea} in the north of 20°N along 137°E is attributable mainly to the uptake of anthropogenic CO_2 in the surface water (Fig. 9), consistent with observations (Midorikawa *et al*., 2005). On the other hand, the model results show that the increase of pCO_{2sea} to the south of 20°N along 137°E is attributable mainly to the regional increase in SST. The effect of SST on the pCO_{2sea} increase is much more dominant in wider domains in the model than that estimated by the observation (Midorikawa *et al*., 2005). This is due to a greater increase in SST from 1990 to 2004 in the model than in the observations. Along 155°W, the increase in pCO_{2sea} is caused mainly by the regional change in DIC at all latitudes, owing to invasion of the anthropogenic CO_2 in the surface waters (Fig. 9). The increase in pCO_{2sea} is partly compensated for by a decrease in SST over the entire region.

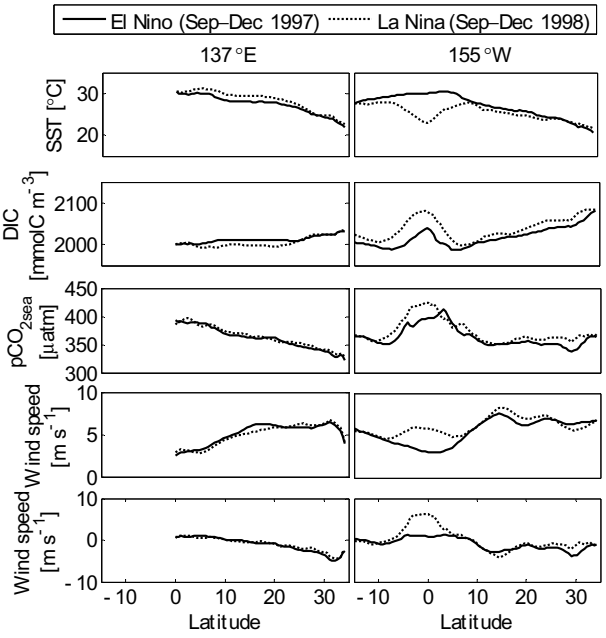

Fig. 10. Modeled latitudinal profiles of SST, SSS, surface DIC and TA, pCO_{2sea}, wind speed and sea-to-air CO_2 flux, along 137°E and 155°W, in September–December 1997 (El Niño period; solid lines) and September–December 1998 (La Niña period; dotted lines).

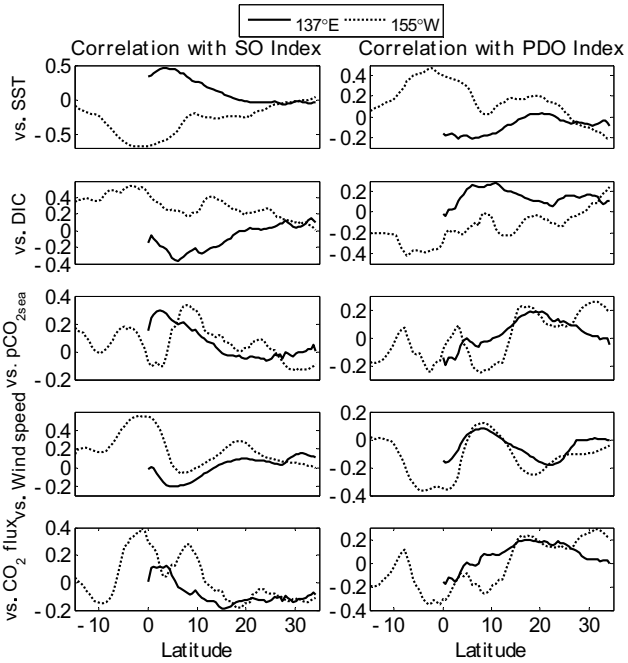

Fig. 11. Modeled latitudinal profiles of correlations of SST, surface DIC, pCO_{2sea}, wind speed and sea-to-air CO_2 flux, with SO or PDO Index (with no time lag), along 137°E (solid lines) and 155°W (dotted lines).

4.2 pCO_{2sea} variation by the El Niño Southern Oscillation and the Pacific Decadal Oscillation

The interannual variability encompasses significant increases in SST and decreases in SSS, DIC, pCO_{2sea}, wind speed and sea-to-air CO_2 flux in the tropical regions along 155°W in 1997–1998, induced by the strongest El Niño of the 20th century (Fig. 5-1). This is consistent with previous studies that show substantial interannual variability in pCO_{2sea} and air–sea CO_2 flux which is strongly correlated with the ENSO (e.g. Christian *et al*., 2008). To elucidate the ENSO-induced influences, we compare model results between September–December 1997 (El Niño condition) and September–December 1998 (La Niña condition) along 137°E and 155°W (Fig. 10).

The model results in the tropical regions along 155°W show a notable increase in SST and decreases in DIC, pCO_{2sea}, wind speed and sea-to-air CO_2 flux, in September–December 1997 (Fig. 10), as has been observed (e.g. Inoue *et al*., 2001; Feely *et al*., 2002). There are also high negative correlation (<–0.5) between the SST and the Southern Oscillation Index (SOI), and high positive correlations (>0.5) of DIC, wind speed and sea-to-air CO_2 flux with the SOI, in the tropical regions along 155°W (Fig. 11). Although the decrease in pCO_{2sea} is seen during El Niño in 1997–1998 (Fig. 5-1), the correlation of pCO_{2sea} with the SOI is not strong (Fig. 11). This is because increase in SST and decrease in DIC counteract each other to diminish significant change in pCO_{2sea} during El Niño. The remarkable decrease in sea-to-air CO_2 flux results from decreased wind speed as well as decreased ΔpCO_2 during El Niño, as suggested by Feely *et al*. (2006). Our model results are also consistent with other previous observational and modeling results: during a non-El Niño period in 1995–1996, the flux in the tropical Pacific had an observed maximum of 6.0–6.5 molC $m^{-2}yr^{-1}$, which drops to 0.5–1.5 molC $m^{-2}yr^{-1}$ during the El Niño of 1997–1998 (Fig. 5-1; Chavez *et al*., 1999; McKinley *et al*., 2004).

The model results in the tropical regions along 137°E show that the SOI has a positive correlation with SST, a negative correlation with DIC, and a relatively weak correlation with pCO_{2sea} (Fig. 11). Correlations of the other fields with the SOI are not significant along 137°E (Fig. 11). It is likely that the effect on pCO_{2sea} of increased DIC is counteracted by the effect of decreasing SST, as also mentioned in Midorikawa *et al*. (2005). The total effect is very little change in pCO_{2sea} and air–sea CO_2 flux along 137°E during the 1997/1998 El Niño event (Fig. 10).

We examine the contribution of ΔpCO_2 (pCO_{2sea} minus pCO_{2air}) and wind variability to the air–sea CO_2 flux variability between September–December 1997 (El

Niño condition) and September–December 1998 (La Niña condition). The contribution of the wind is proportional to the square of the wind speed in the model (Wanninkhof, 1992). The model result agrees with previous studies (Boutin *et al*., 1999; Feely *et al*., 2002; McKinley *et al*., 2004) in that unlike in the western and eastern tropical and other oceanic regions, the wind speed variability plays a non-negligible role in driving the interannual air–sea CO_2 flux variability in the central tropical Pacific. However, the contribution of the wind variability to the air–sea CO_2 flux variability in the central tropical Pacific is smaller (~7%) in this study than in a previous modeling study (approximately 30%; McKinley *et al*., 2004).

Mantua *et al*. (1997) defined the PDO index as the leading principal component of observed SST anomalies in the Pacific north of 20°N. Evidence for the regime shift that occurred in 1989 were found more clearly in biological records than in the physical data (Hare *et al*., 2000; Hare and Mantua., 2000). Brix *et al*. (2004) suggested a more pronounced influence of the PDO than the ENSO to interannual variability of the upper ocean carbon cycle at Station ALOHA near Hawaii. Although the effects of the PDO on the physical and biogeochemical processes are considered much smaller and less distinguishable than those of ENSO in the Pacific south of 20°N, Takahashi *et al*. (2003) reported that the mean growth rate of pCO_{2sea} changed from 0.5 ± 0.3 μatm yr^{-1} to 3.4 ± 0.4 μatm yr^{-1} before and after the PDO shift that occurred between 1988 and 1992 in the western and central tropical Pacific between 135°E and 175°E, suggesting a significant acceleration in the pCO_{2sea} growth after the phase shift of the PDO. However, the overall influences of the PDO to the oceanic carbon system in the entire subtropical and tropical Pacific are not elucidated well by observations.

The model results show that the PDO index has a positive correlation with SST and a negative correlation with surface DIC south of 25–30°N along 155°W (Fig. 11). It is interesting that the correlations are reversed north of 25–30°N. Along 137°E, on the other hand, the correlation is similar across latitudes, a negative correlation between the PDO and SST and a positive correlation between the PDO and surface DIC. The opposite effects on pCO_{2sea} of SST and surface DIC, and disparate relationships between the PDO and wind speed in different oceanic regions result in weak overall correlations between the PDO and pCO_{2sea} and between the PDO and air–sea CO_2 flux. Although the correlations are weak, our model results of the effects of the PDO on the pCO_{2sea} and air–sea CO_2 flux are still considered relatively strong. McKinley *et al*. (2006) concluded that air–sea CO_2 flux anomalies are correlated with the PDO, but that interannual to decadal timescale responses of pCO_{2sea} and air–sea CO_2 flux to the PDO are generally amplified in the higher resolution models, such as ours.

5. Conclusion and Remarks

We use a 3-D physical-biogeochemical model to identify the factors that cause seasonal and interannual variations of pCO_{2sea} and air–sea CO_2 flux in the tropical–subtropical Pacific. The model results suggest the following conclusions.

(1) The model reproduces well the observed temporal and spatial variations of the pCO_{2sea} and air–sea CO_2 flux. The model clearly demonstrates relatively higher sea surface temperature (SST), and lower dissolved inorganic carbon (DIC) and pCO_{2sea} in the western than in the central tropical–subtropical Pacific. Seasonal variations are predominant in the subtropical Pacific, while interannual variations, especially driven by the ENSO, are pronounced in the central tropical Pacific.

(2) The net effect of the SST and DIC change accounts for 95% and 76% of the seasonal and interannual pCO_{2sea} change, respectively, in the tropical–subtropical regions. Following the pCO_{2air} increase from 1990 to 2004, the surface DIC has also increased for the entire region. The SST, on the other hand, has increased in the subtropical and western tropical Pacific but has decreased in the central tropical Pacific over the same period. As a result, the response of pCO_{2sea} to the interannual variations is spatially variable. Our model results suggest a non-negligible contribution of the wind variability to the air–sea CO_2 flux in the central tropical Pacific, but the modeled contribution of 7% is much less than that from a previous modeling study (30%; McKinley *et al*., 2004).

(3) For more realistic simulations and future projections of pCO_{2sea} and air–sea CO_2 flux, we need long-term observational data with a fine spatial resolution to resolve physical and biogeochemical processes. Moreover, eddy-permitting ocean models may better reproduce the interannual variability of pCO_{2sea} and its controlling factors, for example, the SSS variability like the substantial freshening that occurred in 1995–1997 at Station ALOHA.

Acknowledgements

We thank three reviewers for providing helpful and constructive comments. M. Fujii was supported by MEXT through Special Coordination Funds for Promoting Sciences and Technology. F. Chai has received supports from NSF and NASA for his modeling work.

References

Anderson, L. A. and J. L. Sarmiento (1994): Redfield rations of remineralization determined by nutrient data analysis. *Global Biogeochem. Cycles*, **8**, 65–80.

Barber, R. T. (1992): Introduction to the WEC88 cruise—an investigation into why the equator is not greener. *J. Geophys. Res*., **97**, 609–610.

Barber, R. T., M. P. Sanderson, S. T. Lindley, F. Chai, J. Newton, C. C. Trees, D. G. Foley and F. P. Chavez (1996):

Primary productivity and its regulation in the equatorial Pacific during and following the 1991–1992 El Niño. *Deep-Sea Res. Part II*, **43**, 933–969.

Boutin, J., J. Etcheto, Y. Dandonneau, D. C. E. Bakker, R. A. Feely, H. Y. Inoue, M. Ishii, R. D. Ling, P. D. Nightingale, N. Metzl and R. Wanninkhof (1999): Satellite sea surface temperature: a powerful tool for interpreting in situ pCO_2 measurements in the equatorial Pacific Ocean. *Tellus*, **51B**, 490–508.

Brix, H., N. Gruber and C. D. Keeling (2004): Interannual variability of the upper ocean carbon cycle at station ALOHA near Hawaii. *Global Biogeochem. Cycles*, **18**, GB4019, doi:10.1029/2004GB002245.

Buitenhuis, E. T. *et al.* (2006): Biogeochemical fluxes through mesozooplankton. *Global Biogeochem. Cycles*, **20**, GB2003, doi:10.1029/2005GB002511.

Chai, F., R. C. Dugdale, T.-H. Peng, F. P. Wilkerson and R. T. Barber (2002): One-dimensional ecosystem model of the equatorial Pacific upwelling system. Part I: model development and silicon and nitrogen cycle. *Deep-Sea Res. Part II*, **49**, 2713–2745.

Chai, F., M. Jiang, R. T. Barber, R. C. Dugdale and Y. Chao (2003): Interdecadal variation of the transition zone chlorophyll front: A physical-biological model simulation between 1960 and 1990. *J. Oceanogr.*, **59**, 461–475.

Chai, F., G. Liu, H. Xue, L. Shi, Y. Chao, C.-M. Tseng, W.-C. Chou and K.-K. Kiu (2009): Seasonal and interannual variability of carbon cycle in South China Sea: A three-dimensional physical-biogeochemical modeling study. *J. Oceanogr.*, **65**, this issue, 703–720.

Chavez, F. P., P. G. Strutton, G. E. Friedrich, R. A. Feely, G. C. Feldman, D. G. Foley and M. J. McPhaden (1999): Biological and chemical response of the equatorial Pacific Ocean to the 1997–98 El Niño. *Science*, **286**, 2126–2131.

Christian, J. R., M. Verschell, R. Murtugudde, A. J. Busalacchi and C. R. McClain (2002): Biogeochemical modeling of the tropical Pacific Ocean: I. Seasonal and interannual variability. *Deep-Sea Res. Part II*, **49**, 509–543.

Christian, J. R., R. A. Feely, M. Ishii, R. Murtugudde and X. Wang (2008): Testing an ocean carbon model with observed sea surface pCO_2 and dissolved inorganic carbon in the tropical Pacific Ocean. *J. Geophys. Res.*, **113**, C07047, doi:10.1029/2007JC004428.

Conway, T. J., K. A. Masarie and N. Zhang (1994): Evidence for interannual variability of the carbon cycle from the National Oceanic and Atmospheric Administration/Climate Monitoring and Diagnostics Laboratory Global Air Sampling Network. *J. Geophys. Res.*, **99**, 22831–22855.

Cosca, C. E., R. A. Feely, J. Boutin, J. Etcheto, M. J. McPhaden, F. P. Chavez and P. G. Strutton (2003): Seasonal and interannual CO_2 fluxes from the central and eastern equatorial Pacific Ocean as determined from fCO_2-SST relationship. *J. Geophys. Res.*, **108**, 3278, doi:10/2000JC000677.

Dore, J. E., R. Lukas, D. W. Sadler and D. M. Karl (2003): Climate-driven changes to the atmospheric CO_2 sink in the subtropical North Pacific Ocean. *Nature*, **424**, 754–757.

Dugdale, R. C., R. T. Barber, F. Chai, T.-H. Peng and F. P. Wilkerson (2002): One-dimensional ecosystem model of the equatorial Pacific upwelling system. Part II: sensitivity analysis and comparison with JGOFS EqPac data. *Deep-Sea Res. Part II*, **49**, 2747–2768.

Dunne, J. P., J. W. Murray, A. K. Aufdenkampe, S. Blain and M. Rodier (1999): Silicon-nitrogen coupling in the equatorial Pacific upwelling zone. *Global Biogeochem. Cycles*, **13**, 715–726.

Feely, R. A., R. Wanninkhof, C. E. Cosca, P. P. Murphy, M. F. Lamb and M. D. Steckley (1995): CO_2 distribution in the equatorial Pacific during the 1991–1992 ENSO event. *Deep-Sea Res. Part II*, **42**, 365–386.

Feely, R. A., R. Wanninkhof, C. Goyat, D. E. Archer and T. Takahashi (1997): Variability of CO_2 distribution and sea-air fluxes in the central and eastern equatorial Pacific during the 1991–1994 El Niño. *Deep-Sea Res. Part II*, **44**, 1851–1867.

Feely, R. A., R. Wanninkhof, T. Takahashi and P. Tans (1999): Influence of El Niño on the equatorial Pacific contribution of atmospheric CO_2 accumulation. *Nature*, **398**, 597–601.

Feely, R. A., J. Boutin, C. E. Cosca, Y. Dandonneau, J. Etcheto, H. Y. Inoue, M. Ishii, C. Le Quéré, D. J. Mackey, M. McPhaden, N. Metzl, A. Poisson and R. Wanninkhof (2002): Seasonal and interannual variability of CO_2 in the equatorial Pacific. *Deep-Sea Res. Part II*, **49**, 2443–2469.

Feely, R. A., R. Wanninkhof, W. McGillis, M.-E. Carr and C. E. Cosca (2004): Effects of wind speed and gas exchange parameterizations on the air-sea CO_2 fluxes in the equatorial Pacific Ocean. *J. Geophys. Res.*, **109**, C08S03, doi:10.1029/2003JC001896.

Feely, R. A., T. Takahashi, R. Wanninkhof, M. J. McPhaden, C. E. Cosca, S. C. Sutherland and M.-E. Carr (2006): Decadal variability of the air-sea CO_2 fluxes in the equatorial Pacific Ocean. *J. Geophys. Res.*, **111**, C08S90, doi:10.1029/2005JC003129.

Foley, D. G., T. D. Dickey, M. J. McPhaden, R. R. Bidigare, M. R. Lewis, R. T. Barber, S. T. Lindley, C. Garside, D. V. Manov and J. D. McNeil (1996): Long waves and primary productivity variations in the equatorial Pacific at 0°N, 140°W. *Deep-Sea Res. Part II*, **44**, 1801–1826.

Fujii, M. and F. Chai (2007): Modeling carbon and silicon cycling in the equatorial Pacific. *Deep-Sea Res. Part II*, **54**, 496–520.

Fujii, M. and Y. Yamanaka (2008): Effects of storms on primary productivity and air-sea CO_2 exchange in the subarctic western North Pacific: a modeling study. *Biogeosciences*, **5**, 1189–1197.

Hare, S. R. and N. J. Mantua (2000): Empirical evidence for North Pacific regime shifts in 1977 and 1989. *Prog. Oceanogr.*, **47**, 103–145.

Hare, S. R., S. Minobe, W. S. Wooster and S. McKinnell (2000): An introduction to the PICES symposium on the nature and impacts of North Pacific climate regime shifts. *Prog. Oceanogr.*, **47**, 99–102.

Inoue, H. Y., Y. Sugihara and K. Fushimi (1987): pCO_2 and $\delta^{13}C$ in the air and surface sea water in the western North Pacific. *Tellus*, **39B**, 228–242.

Inoue, H. Y., H. Matsueda, M. Ishii, K. Fushimi, M. Hirota, I. Asanuma and Y. Takasugi (1995): Long-term trend of the partial pressure of carbon dioxide (pCO_2) in surface waters of the western North Pacific, 1984–1993. *Tellus*, **47B**, 391–

413.
Inoue, H. Y., M. Ishii, H. Matsueda, M. Aoyama and I. Asanuma (1996): Changes in longitudinal distribution of the partial pressure of CO_2 (pCO_2) in the central and western equatorial pacific, west of 160°W. *Geophys. Res. Lett.*, **23**, 1781–1784.
Inoue, H. Y., M. Ishii, H. Matsueda, S. Saito, M. Aoyama, T. Tokieda, T. Midorikawa, K. Nemoto, T. Kawano, I. Asanuma, K. Ando, T. Yano and A. Murata (2001): Distributions and variations in the partial pressure of CO_2 in surface waters (pCO_2^w) of the central and western equatorial Pacific during the 1997/1998 El Niño event. *Mar. Chem.*, **76**, 59–75.
Ishii, M. and H. Y. Inoue (1995): Air-sea exchange of CO_2 in the central and western equatorial Pacific in 1990. *Tellus*, **47B**, 447–460.
Ishii, M., H. Y. Inoue, H. Matsueda, S. Saito, K. Fushimi, K. Nemoto, T. Yano, H. Nagai and T. Midorikawa (2001): Seasonal variation in total inorganic carbon and its controlling processes in surface waters of the western North Pacific subtropic gyre. *Mar. Chem.*, **75**, 17–32.
Ishii, M., S. Saito, T. Tokieda, T. Kawano, K. Matsumoto and H. Y. Inoue (2004): Variability of surface layer CO_2 parameters in the western and central equatorial Pacific. p. 59–94. In *Global Envionmental Change in the Ocean and on Land*, ed. by M. Shiyomi *et al.*, Terrapub, Tokyo.
Ishii, M., H. Y. Inoue, T. Midorikawa, S. Saito, T. Tokieda, D. Sasano, A. Nakadate, K. Nemoto, N. Metzl, C. S. Wong and R. A. Feely (2009): Spatial variability and decadal trend of the oceanic CO_2 in the western equatorial Pacific warm/fresh water. *Deep-Sea Res. Part II*, **56**, 591–606.
Jiang, M.-S. and F. Chai (2005): Physical and biological controls on the latitudinal asymmetry of surface nutrients and pCO_2 in the central and eastern equatorial Pacific. *J. Geophys. Res.*, **110**, C06007, doi:10.1029/2004JC002715.
Jiang, M.-S. and F. Chai (2006): Physical control on the seasonal cycle of surface pCO_2 in the equatorial Pacific. *Geophys. Res. Lett.*, **33**, L23608, doi:10.1029/2006GL027195.
Kalnay, E., M. Kanamitsu, R. Kistler, W. Collins, D. Deaven, L. Gandin, M. Iredell, S. Saha, G. White, J. Woollen, Y. Zhu, M. Chelliah, W. Ebisuzaki, W. Higgins, J. Janowiak, K. C. Mo, C. Ropelewski, J. Wang, A. Leetmaa, R. Reynolds, R. Jenne and D. Joseph (1996): The NCEP/NCAR 40-year reanalysis project. *Bull. Am. Meteorol. Soc.*, **77**, 437–471.
Karl, D. M. and R. Lukas (1996): The Hawaii Ocean Time-series (HOT) program: Background, rationale and field implementation. *Deep-Sea Res. Part II*, **43**, 129–156.
Keeling, C. D., R. B. Bacastow and T. P. Whorf (1982): Measurements of the concentration of carbon dioxide at Mauna Loa Observatory, Hawaii. In *Carbon Dioxide Review*, ed. by W. C. Clark, Oxford Univ. Press, New York.
Keeling, C. D., H. Brix and N. Gruber (2004): Seasonal and long-term dynamics of the upper ocean carbon cycle at Station ALOHA near Hawaii. *Global Biogeochem. Cycles*, **18**, GB4006, doi:10.1029/2004GB002227.
Le Borgne, R., R. A. Feely and D. J. Mackey (2002): Carbon fluxes in the equatorial Pacific: a synthesis of the JGOFS programme. *Deep-Sea Res. Part II*, **49**, 2425–2442.
Le Quéré, C., J. C. Orr, P. Monfray and O. Aumont (2000): Interannual variability of the oceanic sink of CO_2 from 1979 through 1997. *Global Biogeochem. Cycles*, **14**, 1247–1265.
Liu, G. and F. Chai (2009): Seasonal and interannual variation of physical and biological processes during 1994–2001 in the Japan/East Sea: a three-dimensional physical-biogeochemical modeling study. *J. Mar. Syst.*, doi:10.1016/j.jmarsys.2009.02.011 (in press).
Mantua, N. J., S. R. Hare, Y. Zhang, J. M. Wallace and R. C. Francis (1997): A Pacific interdecadal climate oscillation with impacts on salmon production. *Bull. Am. Meteorol. Soc.*, **78**, 1069–1079.
McKinley, G. A., M. J. Follows and J. Marshall (2004): Mechanisms of air-sea CO_2 flux variability in the equatorial Pacific and the North Atlantic. *Global Biogeochem. Cycles*, **18**, GB2011, doi:10.1029/2003GB002179.
McKinley, G. A., T. Takahashi, E. Buitenhuis, F. Chai, J. R. Christian, S. C. Doney, M.-S. Jiang, K. Lindsay, J. K. Moore, C. Le Quéré and I. Lima (2006): North Pacific carbon cycle response to climate variability on seasonal to decadal timescales. *J. Geophys. Res.*, **111**, C07S06, doi:1029/2005JC003173.
Midorikawa, T., K. Nemoto, H. Kamiya, M. Ishii and H. Y. Inoue (2005): Persistently strong oceanic CO_2 sink in the western subtropical North Pacific. *Geophys. Res. Lett.*, **32**, L05612, doi:10.1029/2004GL021952.
Millero, F. J., K. Lee and M. Roche (1998): Distribution of alkalinity in the surface waters of the major oceans. *Mar. Chem.*, **60**, 111–130.
Moore, J., S. Doney and K. Lindsay (2004): Upper ocean ecosystem dynamics and iron cycling in a global three-dimensional model. *Global Biogeochem. Cycles*, **18**, GB4028, doi:10.1029/2004GB002220.
Murata, A. and K. Fushimi (1996): Temporal and spatial variations in atmospheric and oceanic CO_2 in the western North Pacific from 1990 to 1993: Possible link to the 1991/92 ENSO event. *J. Meteorol. Soc. Japan*, **74**, 1–20.
Obata, A. and Y. Kitamura (2003): Interannual variability of the sea-air exchange of CO_2 from 1961 to 1998 simulated with a global ocean circulation-biogeochemistry model. *J. Geophys. Res.*, **108**, 3337, doi:1029/2001JC001088.
Orr, J. C. (1996): The Ocean Carbon-Cycle Intercomparison Project of IGBP/GAIM. p. 33–52. In *Ocean Storage of Carbon Dioxide*, ed. by W. Ormerod, IEA Greenhouse R&D Programme, Workshop 3—International Links and Concerns, ISBN 1 898373 04 3, CRE Group Ltd., Cheltenham GL52 4RZ, U.K.
Park, G.-H., K. Lee, R. Wanninkhof and R. A. Feely (2006): Emperical temperature-based estimates of variability in the oceanic uptake of CO_2 over the past 2 decades. *J. Geophys. Res.*, **111**, C07S07, doi:10.1029/2005JC003090.
Takahashi, T., J. Olafsson, J. G. Goddard, D. W. Chipman and S. C. Sutherland (1993): Seasonal variation of CO_2 and nutrients in the high-latitude surface oceans: A comparative study. *Global Biogeochem. Cycles*, **7**, 843–878.
Takahashi, T., R. Feely, R. F. Weiss, R. H. Wanninkhof, D. W. Chipman, S. C. Sutherland and T. T. Takahashi (1997): Global air-sea flux of CO_2: An estimate based on measurements

of sea-air pCO_2 difference. *Proc. Natl. Acad. Sci. USA*, **94**, 8292–8299.

Takahashi, T., R. H. Wanninkhof, R. A. Feely, R. F. Weiss, D. W. Chipman, N. Bates, J. Olafsson, C. Sabine and S. C. Sutherland (1999): Net sea-air CO_2 flux over the flobal oceans: An improved estimate based on the sea-air pCO_2 difference. p. 9–15. In *Proceedings of the 2nd International Symposium CO_2 in the Oceans*, Tsukuba, January 1999, CGER-I037-'99, CGER/NIES.

Takahashi, T., S. C. Sutherland, C. Sweeney, A. Poisson, N. Metzl, B. Tilbrook, N. Bates, R. Wanninkhof, R. A. Feely, C. Sabine, J. Olafsson and Y. Nojiri (2002): Global sea-air CO_2 flux based on climatological surface ocean pCO_2, and seasonal biological and temperature effects. *Deep-Sea Res. Part II*, **49**, 1601–1622.

Takahashi, T., S. C. Sutherland, R. A. Feely and C. E. Cosca (2003): Decadal variation of the surface water pCO_2 in the western and central equatorial Pacific. *Science*, **302**, 852–856.

Takahashi, T., S. C. Sutherland and A. Kozyr (2008): Global ocean surface water partial pressure of CO_2 database: Measurements performed during 1968–2006 (Version 1.0). ORNL/CDIAC-152, NDP-088. Carbon Dioxide Information Analysis Center, Oak Ridge National Laboratory, U.S. Department of Energy, Oak Ridge, TN 37831, 20 pp.

Takahashi, T., S. C. Sutherland, R. Wanninkhof, C. Sweeney, R. A. Feely, D. W. Chipman, B. Hales, G. Friederich, F. Chavez, A. Watson, D. C. E. Bakker, U. Schuster, N. Metzl, H. Yoshikawa-Inoue, M. Ishii, T. Midorikawa, Y. Nojiri, C. Sabine, J. Olafsson, Th. S. Arnarson, B. Tilbrook, T. Johannessen, A. Olsen, R. Bellerby, A. Körtzinger, T. Steinhoff, M. Hoppema, H. J. W. de Baar, C. S. Wong, B. Delille and N. R. Bates (2009): Climatological mean and decadal changes in surface ocean pCO_2, and net sea-air CO_2 flux over the global oceans. *Deep-Sea Res. Part II*, **56**, 554–577.

Tans, P. P., I. Y. Fung and T. Takahashi (1990): Observational constraints on the global atmospheric CO_2 budget. *Science*, **247**, 1431–1438.

Toggweiler, J. R. and S. Carson (1995): What are upwelling systems contributing to the oceans's carbon and nutrient budgets? p. 337–360. In *Upwelling in the Ocean: Modern Processes and Ancient Records*, ed. by C. P. Summerhayes, K.-C. Emeis, M. V. Angel, R. L. Smith and B. Zeitzschel, John Wiley, New York.

Wang, X. and Y. Chao (2004): Simulated sea surface salinity variability in the tropical Pacific. *Geophys. Res. Lett.*, **31**, L02302, doi:10.1029/2003GLD18146.

Wang, X., J. R. Christian, R. Murtugudde and A. J. Busalacchi (2006): Spatial and temporal variability of the surface water pCO_2 and air-sea CO_2 flux in the equatorial Pacific during 1980–2003: A basin-scale carbon cycle model. *J. Geophys. Res.*, **111**, C07S04, doi:10.1029/2005JC002972.

Wanninkhof, R. (1992): Relationship between wind speed and gas exchange. *J. Geophys. Res.*, **97**, 7373–7382.

Wetzel, P., A. Winguth and E. Maier-Reimer (2005): Sea-to-air CO_2 flux from 1948 to 2003: A model study. *Global Biogeochem. Cycles*, **19**, GB2005, doi:10.1029/2004GB002339.

Winguth, A. M. E., M. Heimann, K. D. Kurz, E. Maier-Reimer, U. Mikolajewicz and J. Segschneider (1994): El Niño-Southern Oscillation related fluctuations of the marine carbon cycle. *Global Biogeochem. Cycles*, **8**, 39–63.

*This paper is a consolidation of two presentations at the Topic Session on "Decadal changes in carbon biogeochemistry in the North Pacific" convened at the PICES Sixteenth Annual Meeting in Victoria, Canada, October 2007.